Elastic scattering of polarized light in multiply domained KH_2PO_4

G. Kh. Kitaeva, S. P. Kulik, A. N. Penin, and A. V. Belinsky
Department of Quantum Radiophysics, Moscow State University 119899, Moscow, Russia
(Received 12 May 1994; revised manuscript received 31 August 1994)

The frequency angular spectra of visible polarized light transmission through multiply domained ferroelectric KH_2PO_4 have been studied. The spectra consist of alternating lines of intensity maxima. The relative intensity and frequency shift between the lines are sensitive to the variations of the domain structure. The known models of anisotropic diffraction by domain walls cannot explain the whole set of unusual characteristics obtained in the experiment, such as the high degree of spectrum regularity, large depolarization of light (up to 70%), and interference between the crossing lines. An interference polarization model is suggested: we consider the combination of transverse-longitudinal-transverse domain blocks with nonregular periodic structure. The analytic and computer simulations show the ability of this model to explain the effects observed in our experiment.

I. INTRODUCTION

The problem of the transmission spectra of multiply domained KH_2PO_4 crystals is far from being new—it attracted attention in the 1960s (Refs. 1,2) and 1970s.[3,4] The effect of intensity modulation of the monochromatic radiation transmitted through ferroelectric crystals of KH_2PO_4 and deuterated KH_2PO_4 has been described by Hill, Hermann, and Ichiki.[1,2] Frequency modulation has been observed in Raman spectra of multiply domained KH_2PO_4.[3] The observed effects are explained by means of one and the same approach: interaction between two orthogonally polarized radiation modes on their way through the regular transverse-domain systems.[1–4] The most complete description of this model was presented by Takagi and Shigenari.[4]

Later we also discovered some peculiarities in the polariton light-scattering spectra of KH_2PO_4.[5,6] These peculiarities make the spectra of multiply domained and monodomain samples look completely different. Such a difference may be caused by the effects described in Refs. 1–4. To find this out, we also turned to the study of the linear transmission spectra of multiply domained KH_2PO_3. We used the method of frequency angular transmission spectra (see Sec. II) which provides detailed information about the parameters of the transmitted radiation. As a result, some features of transmission have been observed which cannot be explained in terms of the models developed previously.[1–4] Analyzing the possible origin of these effects, we came to the conclusion that the traditional model describing the transmission spectra of the crystal domain superlattice needs some correction.

Although the problem is rather old, the effects of light propagation in a crystal with KH_2PO_4-type structure seem to be important. Structures of this kind are widely used in various areas of solid-state physics, nonlinear optics, etc.[7,8] We need to understand completely the basic linear effects of electromagnetic-wave propagation through a superlattice with symmetry of this type.

II. OBSERVATION

Ferroelectric domains in KH_2PO_4 are obtained by cooling the samples below 123 K.[9] Below the Curie temperature the crystal has orthorhombic $mm2$ symmetry (its symmetry above the Curie temperature is tetragonal, $\bar{4}2m$) and the crystallographic X' and Y' axes are directed at the angle 45° to the tetragonal axes and X and Y (Fig. 1). The directions of the Z' axes of neighboring domains are opposite to each other. The domains have the shape of plane layers, their thicknesses being in the range of 5–20 μm (in cases when the process of domain creation under cooling occurs in a mechanically free sample, without any external electrostatic-field application). Usually there are two equally probable domain systems—one of them with domain walls perpendicular to the tetragonal X axis and another one with the walls perpendicular to the tetragonal Y axis. In all cases the domain walls

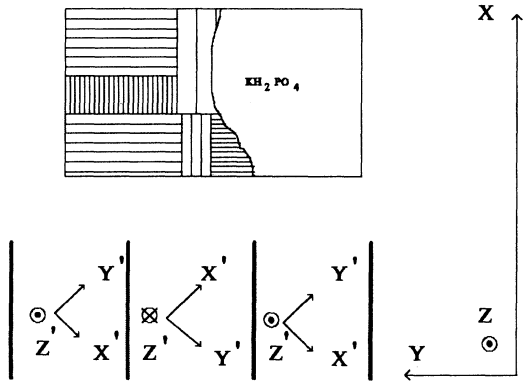

FIG. 1. Schematic picture of domain structure and principal-axis orientation in ferroelectric KH_2PO_4. One can see transverse- and longitudinal-domain blocks.

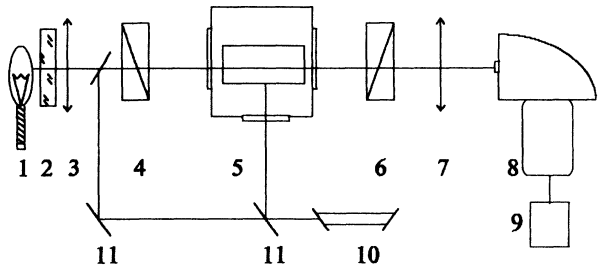

FIG. 2. Setup scheme for investigation of elastic scattering spectra: 1, a tungsten lamp; 2, diffuser; 3,7, lenses; 4, polarizer; 5, the crystal in cryostat; 6, analyzer; 8, spectrograph; 9, registration system; 10, He-Ne laser; 11, mirrors.

contain the Z axis. Domains in the crystal can be arranged in blocks of parallel consecutive domains of approximately the same thickness. In neighboring domains the directions of the X' and Y' axes interchange.[10–12]

Figure 2 shows the experimental setup used for the investigation of the frequency angular transmission spectra. The samples of KH_2PO_4, cut in the form of a rectangular parallelepiped with edges along the tetragonal axes, were placed into a nitrogen cryostat. The domain structure was controlled by the diffraction of He-Ne laser (10) radiation in two directions: along the tetragonal X axis and along the Y axis. A static electric field (0±4 kV/cm) was applied along the polar Z axis to create a single domain or to vary domain thicknesses in the sample (5). The il-

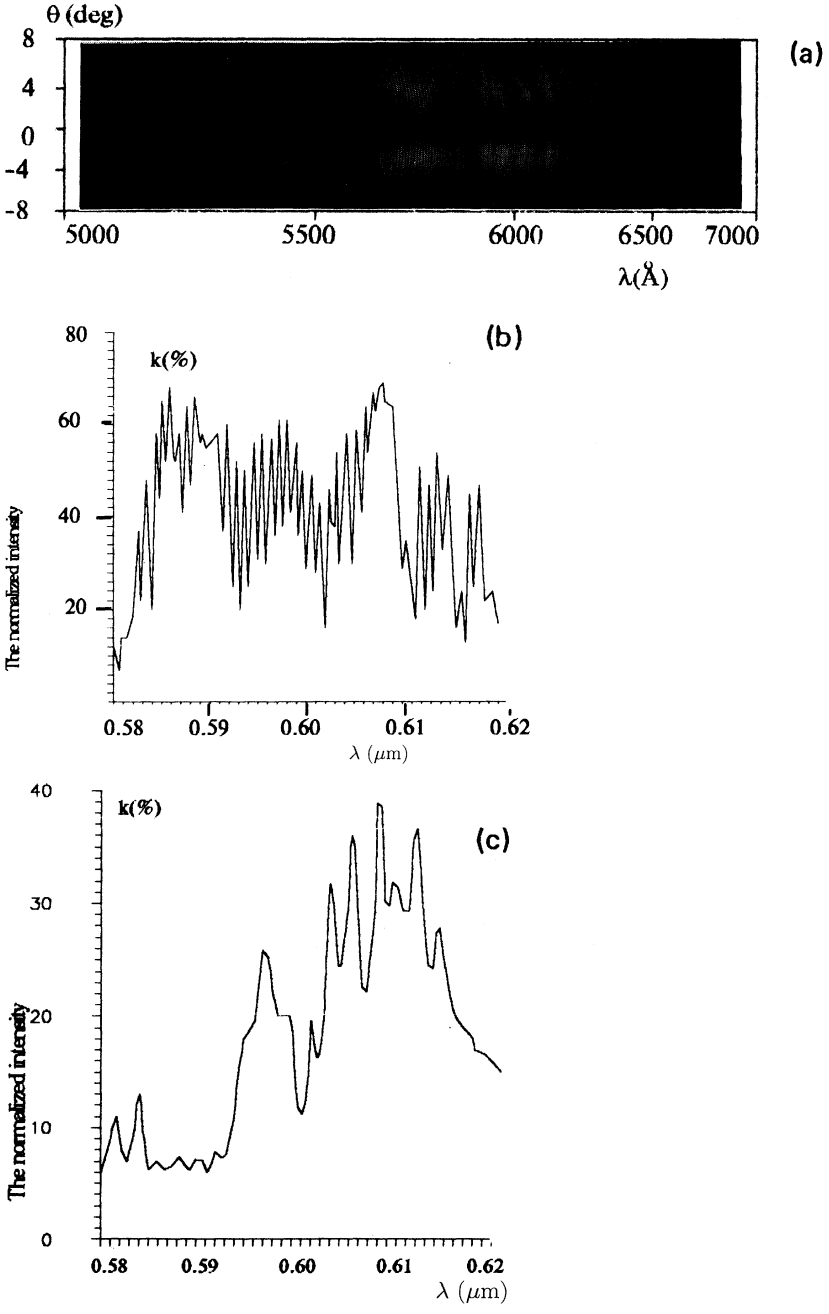

FIG. 3. (a) Photograph of light elastic-scattering spectra in a multiply domained sample (the length $l=30$ mm). (b), (c) Wavelength dependences of the scattering intensity normalized by the input intensity for spectral range 0.58–0.62 μm: $\theta=6°$, $l=30$ mm (b), $\theta=3°$, $l=5$ mm (c).

lumination system consisted of a tungsten lamp (1), a diffuser (2), a short-focus lens (3), and a polarizer—a Glan-Thompson prism (4). It formed a polarized beam of white light diverging in the limits of $\pm 10°$ around the tetragonal X (or Y) axis in the XZ (or YZ) plane. The method of crossed frequency–angular dispersion was applied to obtain the scattering spectra.[13] The light transmitted through the crystal (5) and the analyzer (6) was focused by the lens (7) on the spectrograph slit. It is the essential detail of this registration method that the spectrograph slit is placed in the focal plane of the lens (7). So parallel light beams propagating after the crystal in the same direction (at the angle of inclination θ with respect to the lens optical axis) are focused on the slit surface in circles, the radius of each circle being proportional to $\tan\theta$. The part of the light being cut off by the slit is focused at the exit of the spectrograph camera (8). There the deflection of the focused beam along the slit corresponds to the angle θ and the deflection perpendicular to the slit corresponds to the wavelength of the transmitted light. The two-dimensional spectra of transmitted light in coordinates of wavelength (λ) vs angle (θ) were recorded after the spectrograph either on a photographic film or by a photoelectronic system (9).

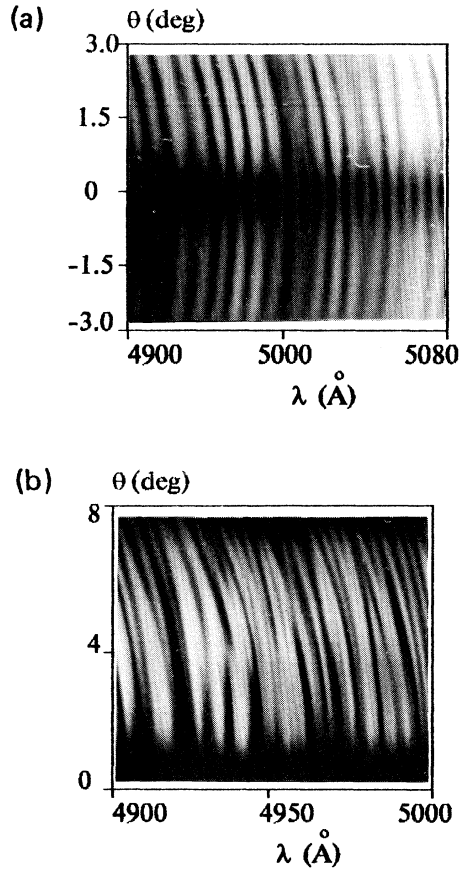

FIG. 4. Fragments of frequency-angular spectra (a) at small angles ($l=5$ mm) and (b) in the case of mutually repulsive lines ($l=30$ mm).

One of the photographs of the scattering spectra of the multiply domained crystal is represented in Fig. 3(a) and the corresponding normalized-light-intensity dependence on the wavelength is represented in Fig. 3(b) for a part of the spectrum. The length of the crystal was 30 mm. The analogous fragment is presented in Fig. 3(c) for a 5 mm length of the crystal.

The represented data were obtained in conditions when the polarization of the radiation under registration was oriented in the crystal ZY plane (e polarization) and the registered waves propagated in the same plane, the crystal being illuminated by white light linearly polarized along the X axis (o polarization). The photographs of parts of other observed spectra are represented in Figs. 4(a) and 4(b).

III. ANALYSIS OF THE EXPERIMENTAL SPECTRA

The discussed transmission spectra of the multiply domained crystal in crossed polarizers are characterized by the following features.

(1) The intensity of the output light with the polarization orthogonal to the input-light polarization depends strongly on the wavelength and the angle of observation. The multiply domained crystal spectrum obtained with the polarizer and analyzer parallel is complementary to the spectrum with crossed polarizers: the intensity maxima and minima interchange.

(2) The spectra are very sensitive to the variation of domain structure. The structure of the domain subsystem was modified by means of an external static field, by changing the observation section, or by taking a sample of another thickness. In the case of the crystal orientation described above, there is no output radiation of orthogonal polarization for a monodomain crystal.

(3) Basically frequency angular spectra consist of alternating lines of intensity maxima with definite curvatures $\rho(\omega)=d\theta/d\omega$ in frequency (ω) and angle (θ) coordinates. In each spectrum we have observed one or a number of line systems, each system containing uncrossing lines with approximately the same curvature. The averaged envelope of these intensity maxima is quasiperiodic. The curvature of lines in a system depends weakly on the domain subsystem structure, being in general a function of frequency. When lines of different systems occupy the same frequency region, interference effects of intensity exchange between the crossing lines occur. The intensity of each line does not depend strongly on the angle θ, but at low angles ($\theta<2°$) it decreases rapidly. In some spectra it decreases down to zero; in others we observed a new set of displaced lines in the region of small angles [see Fig. 4(a)].

(4) The frequency angular spectra are rather regular. They consist of almost equidistant sets of lines. Consider Fig. 5, which shows the probability-distribution histograms of the relative mode distance $P(S_n)$, calculated for spectra of samples with different length l. Here n is the number of the line, $S_n=\Delta\nu_n/\overline{\Delta\nu_n}$, $\Delta\nu_n$ is the frequency shift between two neighbor lines, obtained for constant angle ($\theta=6°$), and $\overline{\Delta\nu_n}$ is the average distance for the

spectrum area containing the lines. The frequency ν is measured in cm^{-1}, $\nu = 1/\lambda$.

For each interval of possible values of S_n we calculated the number of lines corresponding to the relative line distances within the chosen interval. This number is plotted on the ordinate as $P(S_n)$. In the case of the longer sample ($l = 30$ mm) about 200 lines were analyzed; in the case of the shorter one ($l = 5$ mm) we treated about 80 lines. The experimental data for different samples were normalized to make the area under the histograms be equal to 1.

There are also curves corresponding to Gauss, Wigner, and Poisson distributions characterized by the same mean parameters in Fig. 5. The normalizing condition for the functions was $\int_0^\infty P(S)dS = 1$.

Figure 6 demonstrates the distribution histogram of the relative scattering coefficient $P(K_n)$, where $K_n = k_n/\bar{k}_n$, $k_n = I_n^\perp/I_n^\parallel$, $I_n^\perp$ is the light intensity of the orthogonal polarization at the output of the multiply domained crystal, and $I_n^\parallel$ is the radiation intensity at the output of a monodomained homogeneous crystal of the same polarization as the illuminating light. Intensities $I_n^\perp$ and $I_n^\parallel$ are measured at the frequency corresponding to the maximum of the nth line in the multiply domained crystal spectrum. Division by $I_n^\parallel$ allows one to exclude the influence of the detecting-system sensitivity to frequency dispersion. $P(K_n)$ is defined and normalized similarly to $P(S_n)$.

As seen from Figs. 5 and 6, both intensity $P(K_n)$ and line-distance $P(S_n)$ distributions are similar. Their characters do not depend strongly on the sample sizes. In the thin ($l = 5$ mm) crystal the width of the relative line-distance distribution is larger than in the crystal of length $l = 30$ mm. The widths of distributions $P(S_n)$ and $P(K_n)$ change slightly when the domain structure is reconstructed with the help of an external field of order of 50 V/cm, applied along the polar Z' axis. However, the maxima of the distribution functions are always realized for $S_n = 1$, $K_n = 1$, i.e., the averages of the line distance and intensity for each spectrum part are the most probable values. Even 50% deviation from the average is less probable by an order of magnitude than the average.

Histograms $P(S_n)$ and $P(K_n)$ cannot be approximated by Poisson distributions for systems with noncorrelating resonance frequencies, or by the Wigner distribution[14] for stochastic systems. It is the Gauss distribution function that best describes the histogram envelopes $P(S)$ and

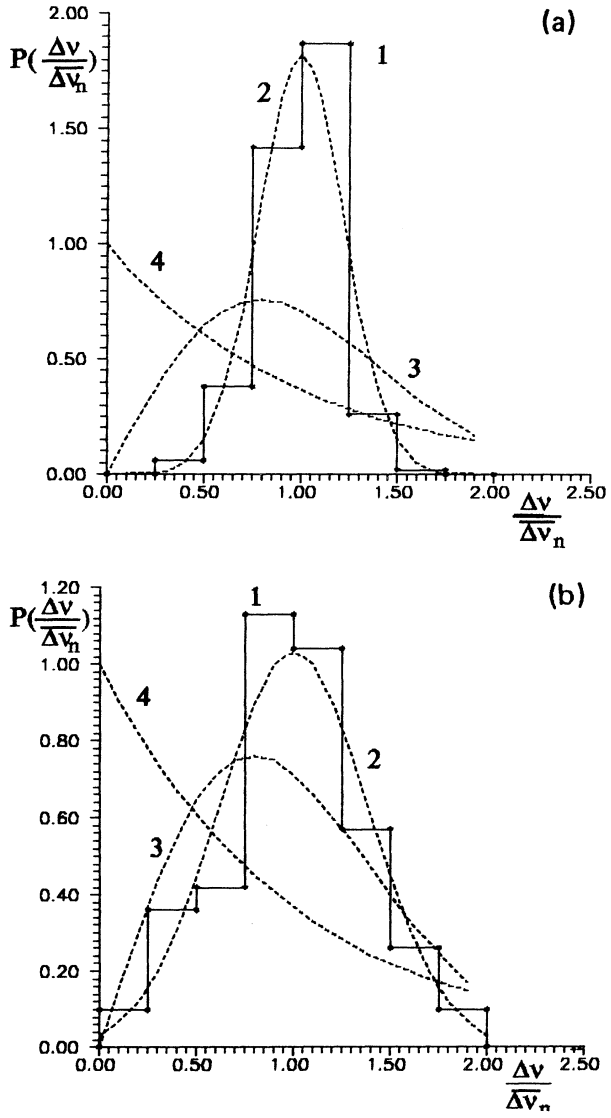

FIG. 5. Distribution functions of relative interline distances in the samples of length $l = 30$ mm (a) and 5 mm (b). 1, measured histograms; 2, Gauss distribution; 3, Wigner distribution; 4, Poisson distribution.

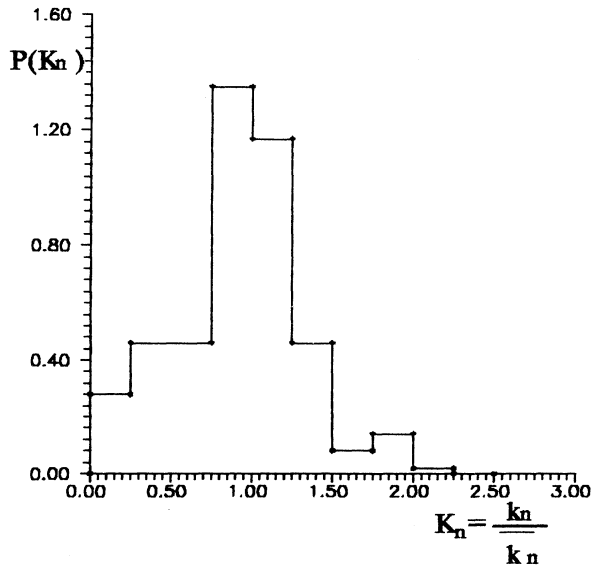

FIG. 6. Distribution function of relative transmission coefficient $P(K_n)$ in the sample of 30 mm length.

$P(K)$.

(5) The average frequency shift $\overline{\Delta\nu_n}$ between the lines increases with increase of the wavelength or with decrease of the sample length. Figure 7(a) shows the approximate spectral distribution of values $1/\overline{\Delta\nu_n}$ in the range of 0.4–0.7 μm. The frequency dependence of the average line density $1/\overline{\Delta\nu_n}$ has a tendency to increase when the frequency rises. This dependence can best be approximated by a first-degree polynomial. The possibility of a linear approximation confirms the two-dimensional character of the scattering system.[14]

(6) The efficiency of conversion from o polarization to e polarization, $\bar{k}$, in the crystals is sufficiently high and can achieve 70%. The average line intensity is not a constant and varies slowly along each spectrum. The variation of $\bar{k}$ has a quasiperiodic character [see Fig. 7(b)]. The value of the period greatly exceeds the frequency shifts between neighboring lines and alters with change of the domain subsystem under illumination. Each maximum of the slow variation of the average intensity contains the group of lines (see Fig. 3).

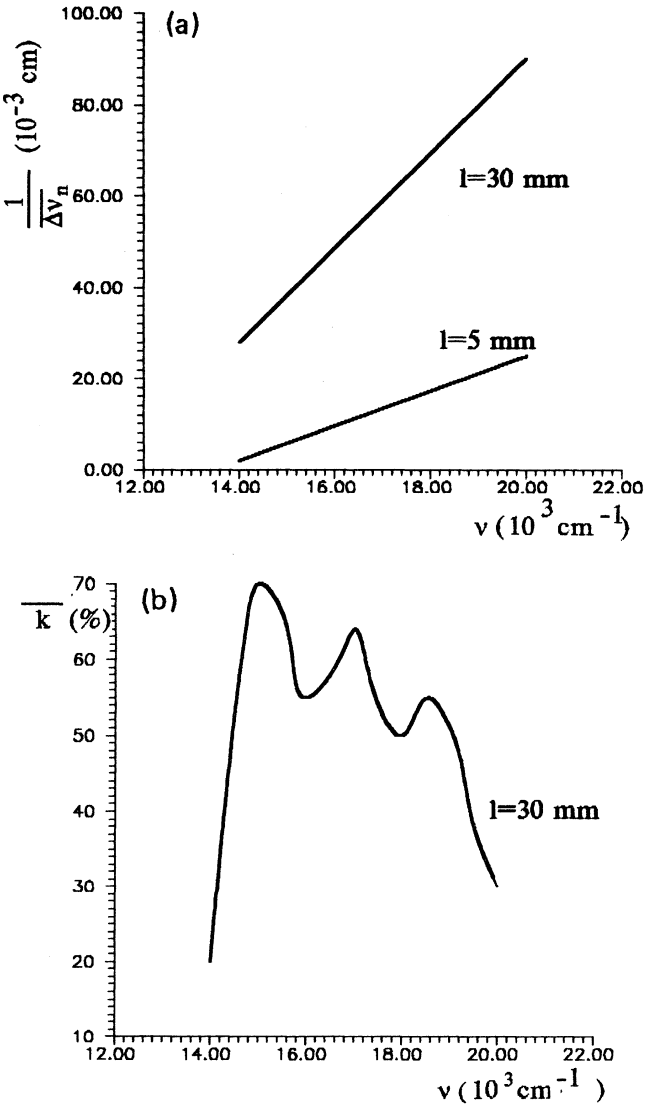

FIG. 7. Spectral dependence of the average line density $1/\overline{\Delta\nu_n}$ (a) and intensity $\bar{k}$ (b).

Finally in this section, we note that the same features are observed in the spectra of deuterated KH_2PO_4. Unfortunately, the domain structure of these crystals is less sensitive to external electric-field variations, so the most detailed investigations were carried out on KH_2PO_4 crystals.

IV. THE EFFECT OF THE TRANSVERSE-DOMAIN BLOCKS

One can select in the domain system of KH_2PO_4-type crystals some blocks consisting of domains with parallel walls (see Fig. 1). The thicknesses of domains in a block are not equal to each other in the general case, but the domain-wall orientation is strictly defined: these walls can be orthogonal to either the X or Y axis. As the light propagates through the crystal, it is scattered by the domain blocks of these two types in sequence. In our experiments we studied either the radiation propagating along the domain walls of one of the block types (we shall call them longitudinal-domain blocks), or the radiation crossing the domain walls of the other type (these blocks will be called transverse).

Let us consider light propagation in an isolated transverse-domain block. We denote the domains with Z' axis directed upwards by the index $+$, and the neighboring domains (with Z' directed downwards) by the index $-$.

If the crystal is illuminated by a plane wave with the wave front parallel to the entrance surface and to the transverse-domain walls, then the light inside the crystal will be split into two components with orthogonal polarizations (denoted as o and e), one of the polarization directions (e) being parallel to the Z axis. We now incline the illuminating wave by angle θ in the plane orthogonal to the plane of Fig. 1. Then the polarization directions will remain orthogonal but will be inclined at angle $\pm\Delta$ with respect to their initial position (Fig. 8). The sign depends on the domain index ($+$ or $-$).[4]

Suppose that in a certain positive ($+$) Nth domain the complex amplitudes of o and e waves are equal to O_N and E_N, respectively. Then, according to Fig. 8(c), the transfer to the negative $(N+1)$th domain corresponds to the unitary transformation

$$\begin{aligned} O_{N+1} &= O_N \cos 2\Delta - E_N e^{i\delta} \sin 2\Delta \ , \\ E_{N+1} &= O_N \sin 2\Delta + E_N e^{i\delta} \cos 2\Delta \ . \end{aligned} \tag{1}$$

Here we chose the o-wave phase as the initial phase, its differences from the e-wave phase being determined by

$$\delta \cong 2\pi d \frac{n_o - n_e}{\lambda \cos(\theta/n_e)} \ , \tag{2}$$

where d is the domain thickness and $n_{o,e}$ the corresponding refractive indices.

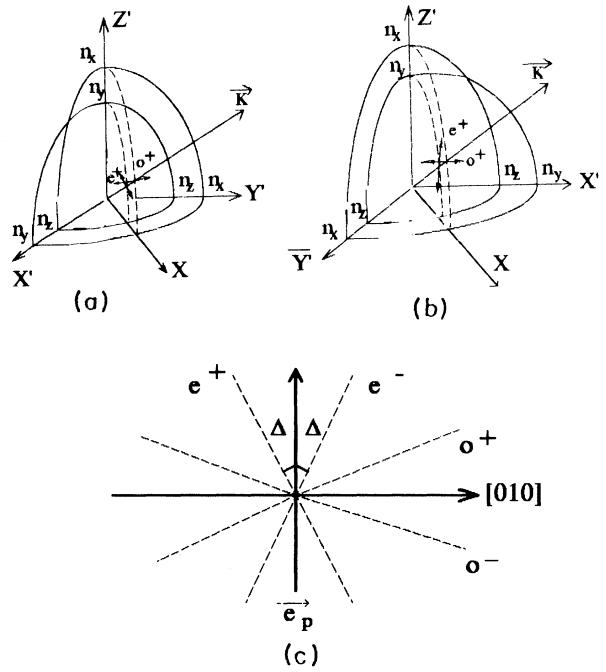

FIG. 8. (a),(b) Refractive-index surfaces of ferroelectric + and − domains in KH_2PO_4; (c) the orientation of the normal wave polarization vectors in the case of propagation in the plane of tetragonal axes Z and X; [010] and e_p correspond to the directions of polarization in the paraelectric phase (Ref. 4).

Note that the situation of nonreflecting domain walls is not an additional assumption. This nontrivial fact follows from the geometry of our experiment, due to the coincidence of the refractive indices of the neighboring domains for the same polarized waves.

The next transformation (from domain − to domain +) has the form

$$O_{N+2}=O_{N+1}\cos2\Delta+E_{N+1}e^{i\delta}\sin2\Delta\ ,$$
$$E_{N+2}=-O_{N+1}\sin2\Delta+E_{N+1}e^{i\delta}\cos2\Delta\ , \tag{3}$$

i.e., it differs from Eq. (1) by the sign of Δ. Thus in the general case

$$\begin{bmatrix}O_{N+1}\\E_{N+1}\end{bmatrix}=\begin{bmatrix}\cos2\Delta & -e^{i\delta}\sin2\Delta\\ \sin2\Delta & e^{i\delta}\cos2\Delta\end{bmatrix}\begin{bmatrix}O_N\\E_N\end{bmatrix}\ ,$$
$$\Delta=(-1)^N|\Delta|\ . \tag{4}$$

These relations enable us to simulate the propagation of light in the domain structure. We shall use them in further numerical calculations. Note that, due to the unitarity of transformation (4) and to a corresponding intensity normalization, the following condition is to be satisfied:

$$|O_N|^2+|E_N|^2=1 \tag{5}$$

for each N. As the estimations show, for $\lambda=0.6\ \mu$m and $T=100$ K we obtain $n_o-n_e\cong0.04$, and at $\theta=6°$ the angle $2\Delta\simeq0.3°$. In spite of such a small value of the orthogonal polarization inclination, the conversion between o and e waves for N large enough can be quite considerable.

If all domains of a transverse block have the same thickness, the minimal element of the periodicity is a component consisting of two domains, the positive (+) and the negative (−) one. This component is described by the matrices (4) for $N=1$ and 2:

$$D^{(2)}\equiv\begin{bmatrix}C & e^{i\delta}S\\ -S & e^{i\delta}C\end{bmatrix}\begin{bmatrix}C & -e^{i\delta}S\\ S & e^{i\delta}C\end{bmatrix}$$
$$=\begin{bmatrix}C^2+e^{i\delta}S^2 & e^{i\delta}(e^{i\delta}-1)CS\\ (e^{i\delta}-1)CS & e^{i\delta}(e^{i\delta}C^2+S^2)\end{bmatrix}\ , \tag{6}$$

where $C\equiv\cos2\Delta$, $S\equiv\sin2\Delta$.

When $\delta=2\pi m$, $m=0,\pm1,\pm2,\ldots$, o and e waves do not interact (N even):

$$D\equiv D^{(N)}\cdots D^{(2)}=D^{(2)}=\begin{bmatrix}1 & 0\\ 0 & 1\end{bmatrix}\ ,$$
$$O_N\equiv O_0\ ,\quad E_N\equiv E_0\ . \tag{7}$$

On the other hand, when $\delta=\pi+2\pi m$,

$$D^{(2)}=\begin{bmatrix}\cos4\Delta & \sin4\Delta\\ -\sin4\Delta & \cos4\Delta\end{bmatrix}\ ,$$
$$D^{(N)}=\begin{bmatrix}\cos2N\Delta & \sin2N\Delta\\ -\sin2N\Delta & \cos2N\Delta\end{bmatrix}\ . \tag{8}$$

Suppose that the radiation in the initial domain is linearly polarized along the o direction:

$$\begin{bmatrix}O_0\\E_0\end{bmatrix}=\begin{bmatrix}1\\0\end{bmatrix}\ . \tag{9}$$

Then the interaction between the o and e waves is most effective (see Fig. 9) for the optimal phase $\delta=\pi+2\pi m$ (for example, $\delta\simeq\pi$ for $\lambda=0.6\ \mu$m, $d=7.5\ \mu$m):

$$O_N=\cos2N\Delta\ ,\quad E_N=-\sin2N\Delta\ , \tag{10}$$

i.e. the amplitudes have harmonic dependence on N and remain real. For the last condition to be valid it is enough that Eq. (9) together with the requirement $\delta=\pi m$ are satisfied for integer m.

It is seen from Fig. 9 that 300 layer domains entirely

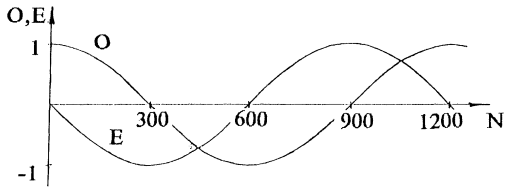

FIG. 9. Evolution of o- and e-wave amplitudes during propagation through N transverse-domain layers calculated for $d=7.5\ \mu$m, $\lambda=0.6\ \mu$m.

transfer the whole energy from the o to the e wave, i.e., rotate the polarization plane of the incident radiation by 90°. As an analogy, one can mention the Zeno paradox formulation by Peres.[15]

The effect of the entire energy transfer from o to e wave can be described in terms of anisotropic diffraction of light.[16] The intensity of the orthogonally polarized light achieves its maximum value when the wave vectors of input wave $\mathbf{k}^{\text{in}}$ and output wave $\mathbf{k}^{\text{out}}$ are connected by the kinematic equation

$$\mathbf{k}^{\text{out}}=\mathbf{k}^{\text{in}}+m\mathbf{q}\ , \tag{11}$$

where $\mathbf{q}=2\pi\mathbf{n}/d$ is the vector of a one-dimensional domain superlattice, $\mathbf{n}$ is the unit vector normal to the domain walls, and m is an integer. It is this effect, arising when the light propagates through a system of transverse domains, which was considered by the authors of Refs. 1–4 and used for the explanation of their experimental spectra. However, the analysis of our experimental data shows that consideration of transverse domains of equal thickness is not enough for the explanation of the observed spectra.

Let us compare the characteristics of our experimental spectra with those predicted by the model described above. The expected line tilts $\rho(\omega)=d\theta/d\omega$ in the frequency angular spectra estimated from Eq. (11) are determined mainly by the known birefringence of the crystal at the given frequency and temperature. Indeed, the curvatures observed in our spectral lines are in good accordance with those calculated from (11). A simple calculation on the basis of (11) shows that the domains having a thickness of order of 10 μm will provide the low-order maxima in the visible range characterized by $m=\pm1$ or not far from it. This is in agreement with the known average domain thickness in KH_2PO_4. Unfortunately, the observed line curvatures and their position in the electromagnetic scale are the only spectral features which can be simply explained by the anisotropic diffraction model.

Let us make an attempt to explain the variety of lines, placed almost equidistantly in the observed spectra, in the framework of Raman-Nath-type diffraction. The regularity of the spectra along the frequency axis could be caused by different orders of diffraction. In this case, the space harmonics of the domain superlattice differing by the value of the inverse lattice vector could correspond to neighboring frequency angular maxima. However the evaluation of $|\mathbf{q}|$ from the relation

$$|\mathbf{q}|=|\mathbf{q}_m|-|\mathbf{q}_{m+1}|=\frac{\Delta n_2(\lambda_2)\lambda_1-\Delta n_1(\lambda_1)\lambda_2}{\lambda_1\lambda_2} \tag{12}$$

(where $\lambda_{1,2}$ are the wavelengths corresponding to the neighboring maxima and $\Delta n_{1,2}$ the effective birefringence in the given direction and temperature at wavelengths $\lambda_{1,2}$) gives a value of domain superlattice period near 1–3 mm for the known crystal birefringence[17,18] in the middle of the visible range at $T=105$ K. This contradicts the data on KH_2PO_4 domain thickness known from literature.[12]

To explain a large number of lines from the point of view of Bragg-type diffraction one must assume that the appearance of each line in a spectrum is caused by diffraction on the corresponding block of subsequent domains of the same thickness. So there must be as many domain blocks in a crystal as there are lines observed in a spectrum, or even more, because our spectra are limited (400–700 nm) and there can be additional lines outside this range. For example, in the case of the spectrum presented in Fig. 3 there must be more than 200 blocks in a sample of 30 mm length. At the same time to provide the high line contrast (the efficiency of conversion from o to e polarization of 50–70 %), it is necessary to have more than 10^2 boundaries, because the efficiency of one boundary is small (10^{-2} in the best case). So, even considering that all domains in the observed part of a crystal have the same orientation perpendicular to the registration-system axis, we came to the conclusion that the crystal length should be more than 10 cm (the domain thickness being of order of 10 μm). Note that in the framework of this model we assume that one domain block forms only one spectral line.

Interpreting the data in Figs. 5 and 6 from the viewpoint of Bragg anisotropic diffraction, we must relate each line frequency (at a given scattering angle) to a corresponding domain thickness, and the interline distances to the differences in thicknesses between domains having the closest transverse sizes. It is seen that the distribution of the relative differences of domain thicknesses is not random and cannot be described by Poisson's law. The Gauss law is the most appropriate for its description. So the distribution of possible domain transverse sizes must be treated as not continuous. As a rule, the domain-thickness difference must be not less than a certain value corresponding to the average line shift. However, there are no other reasons for such extraordinary conclusions about the crystal domain system. There are too many artificial conditions involved for explanation of the observed picture by means of Bragg diffraction by transverse domains. Thus the frequency shifts of the observed lines, their regularity, and the efficient depolarization of the input polarized radiation disagree obviously with the spectra predicted by this model.

V. THE JOINT ACTION OF TRANSVERSE AND LONGITUDINAL DOMAINS

Let us return to relationships (1)–(10) in the case of the optimal phase $\delta=\pm\pi$. We complicate the model, assuming that there is a phase plate Φ (Fig. 10) between two

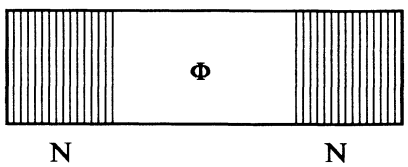

FIG. 10. Schematic picture of three subsequent domain blocks (a "triple"). Φ denotes a phase plate, in particular, a longitudinal-domain block between two transverse-domain blocks.

blocks of 150 transverse domains. This plate adds an additional shift φ to the e-wave phase. If $\varphi=0$ or $2\pi m$, this system is equivalent to a block of 300 domains, which turns the o wave into the e wave. The situation is quite different for $\varphi=(2m+1)\pi$: at $N=150$ the e wave changes its sign (Fig. 9), as if we were at point $N=1050$. After the next 150 layers the field amplitudes achieve their initial values (9). Thus the device shown in Fig. 10, placed between two orthogonal polarizers, is an effective shutter governed by the phase plate Φ. Note that in the absence of transverse domains the phase plate Φ would not influence the radiation with amplitudes (9), for there would be no e wave, and any phase shift φ would produce no effect.

Instead of the phase plate, one can consider a longitudinal-domain block (see Fig. 1) in this device. Indeed, in the described geometry the refractive indices in neighboring longitudinal domains are equal to each other for light propagating at angle θ in the plane parallel to the domain walls. Hence there are no real borders between longitudinal domains of the block for these beams.

The phase shift φ in a longitudinal-domain block can be given by the expression for δ (2), if d is understood, not as a thickness of a single domain, but as a block thickness in the direction normal to the entrance surface of the crystal. In particular, if this length is 3 mm, then $\varphi\simeq 2\pi m$, $m=200$, for $\lambda=0.6$ μm. The neighboring wavelengths, for which also $\varphi=2\pi m$ but $m=199$ and 201, differ from $\lambda=0.6$ μm by approximately 3 nm. Thus, illuminating this device by white light, at first sight we should obtain a spectrum of equidistant lines, similar to that obtained in the experiment (Fig. 3). However, here we forget about the resonant character of the interaction between o and e waves in transverse-domain blocks: the condition $\delta=\pm\pi$ is satisfied only for a certain wavelength, and the next spectral maxima are rather far from the first one.

In order to test this hypothesis, we studied the effect of the phase difference δ on the efficiency of the interaction between o and e waves in a block of transverse domains. The results corresponding to initial polarization (9) are shown in Fig. 11.

The amplitudes O_N and E_N for arbitrary δ are complex. Figure 11 shows the dependences of the e-wave intensity on N for various δ. The dependence of $|E_N|^2$ on δ at fixed N is described by an Airy function,[4,19] its width being $\leq 1°$ in units of the phase deviation from the optimal value $\delta=\pm 180°$, or $\cong 3$ nm in units of the wavelength deviation from the value $\lambda=0.6$ μm. All sets of

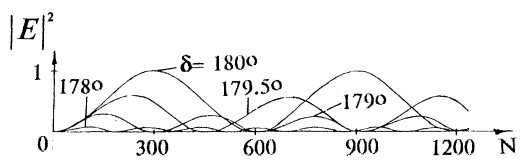

FIG. 11. e-wave intensity dependence on the number of equal transverse domains N for different phase δ.

equidistant lines corresponding to the condition $\varphi=2\pi m$ should occupy only a narrow spectra range, which is determined by the width of the Airy function. However, this contradicts the fact that the experimental spectra contain lines in the whole visible range. Sometimes in experiment it is possible to select a few sets of equidistant lines with slightly differing inclination, but even in such cases each set occupies a spectral interval much wider than the corresponding Airy function.

Thus, taking into account the intermediate blocks of longitudinal domains, we obtain equidistant lines, the distance between them being of the same order as that observed in experiment. Using the typical number of domain walls in the samples investigated, one can also explain the high efficiency of polarization conversion. However, it is necessary to modify this model so as to smooth the resonant character of the interaction between orthogonally polarized waves in transverse-domain blocks.

VI. THE EFFECT OF THE DOMAIN-THICKNESS DISPERSION

Domains in ferroelectric crystals of KH_2PS_4 type do not form an ideal superlattice in each block. Every transverse domain block like the one shown in Fig. 10 can contain domains of different thickness. This must lead to the broadening of the resonant curve of the interaction between two orthogonal polarizations. This is similar to the Airy function broadening due to the random fluctuations of the Fabry-Pérot resonator optical thickness (see, for instance, Refs. 20–22).

Let us consider a modified version of the scheme discussed above. In this version we take into account that the thickness dispersion with respect to the mean value is equal in both transverse blocks. Let there be 200 domains in the first block and 200 in the third one; the mean thickness is $\bar{d}=7.5$ μm. Let the domain thicknesses have a Gaussian distribution with mean square deviation $\sigma\cong 0.2$ μm. A block of longitudinal domains of length 3 mm is placed between two blocks of transverse domains; it acts as a phase plate. Figure 12 shows the results of our numerical calculation for one realization of such a system. It is seen that the one assumption about the slight difference between the domain thicknesses of two transverse blocks enables us to solve (at least partly) the questions that were raised in Sec. V. As a result of this assumption, the number of equidistant lines increases considerably.

Consider the propagation of light which is initially in state (9) through the first block of transverse domains (dashed curves in Fig. 12). The resonance curve $|E_{200}(\lambda)|^2$ is wider than in the case of equal domain thicknesses. This spreading can be estimated in the first approximation in the same way as was done for the random deviations of optical length in the Fabry-Pérot resonator.[20]

Since the Airy function has narrow peaks, corresponding to small deviations of phase, δ, it can be replaced by a Lorentz contour:

$$\frac{1}{1+F\sin^2[(\delta+\Delta\delta)/2]}\cong\frac{1}{1+\frac{1}{4}F(\Delta\delta)^2}\ , \tag{13}$$

where F is the finesse factor of the Airy function, and $\Delta\delta$ the phase deviation from $\delta=\pm\pi$ in radians.

The nth moments of the e-wave intensity distribution can be estimated as

$$\langle |E_N(\delta)|^{2n}\rangle \sim \frac{1}{(2\pi)^{-1}\sigma_\delta}\int_{\infty}^{\infty}\frac{\exp(-\Delta\delta^2/2\sigma_\delta^2)}{[1+\frac{1}{4}F(\delta+\Delta\delta)^2]^n}d(\Delta\delta)\ , \tag{14}$$

where the phase deviation $\Delta\delta$ is connected with the wavelength by means of relationship (2). σ_δ is the mean square phase deviation. The method of analytic calculation of integral (14) is given in the Appendix.

The analytic estimation of the resonance-curve broadening by means of integral (14) for $n=1$ yields a higher value than the results of computer simulation [Fig. 12(a)]. Probably the reason for this fact is that the block of transverse domains with random thicknesses acts both as a converter between o and e polarizations and as a phase plane. Indeed, if a domain is optimal for the conversion (its thickness d and the phases of the interacting waves are optimal), then its border acts as a converter. In the opposite case the domain remains a passive phase plate. Thus, by propagation of light through the whole block, some of the domains are active converters between o and e waves, and some of them can only provide additional phase delays between these waves. There is one more fact confirming this interpretation: the interval between the spectral maxima of the whole system ($\cong$2 nm) is slightly smaller than the value obtained on the assumption that all phase delays are

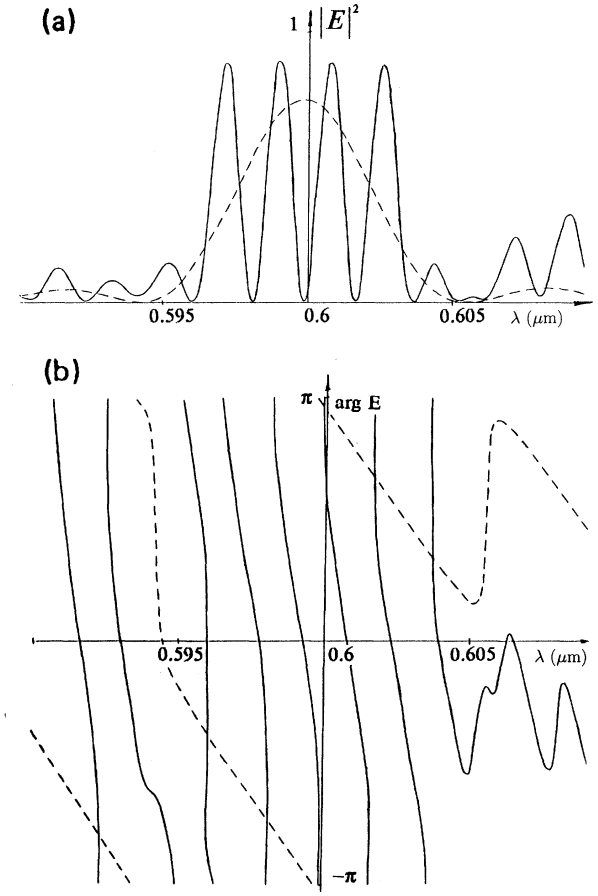

FIG. 12. Calculated spectral distribution of the e-wave intensity (a) and phase (b) after the first block of 200 transverse domains (dashed curve) and the third, 200-domain block (solid curve) for $\theta=6°$. The mean domain thickness in both transverse blocks is $\bar{d}_{1,3}=7.5$ μm, and the mean square deviation of the domain thickness in both transverse blocks is $\sigma_{1,3}=0.185$ μm. The length of the longitudinal block is $d_2=3$ mm.

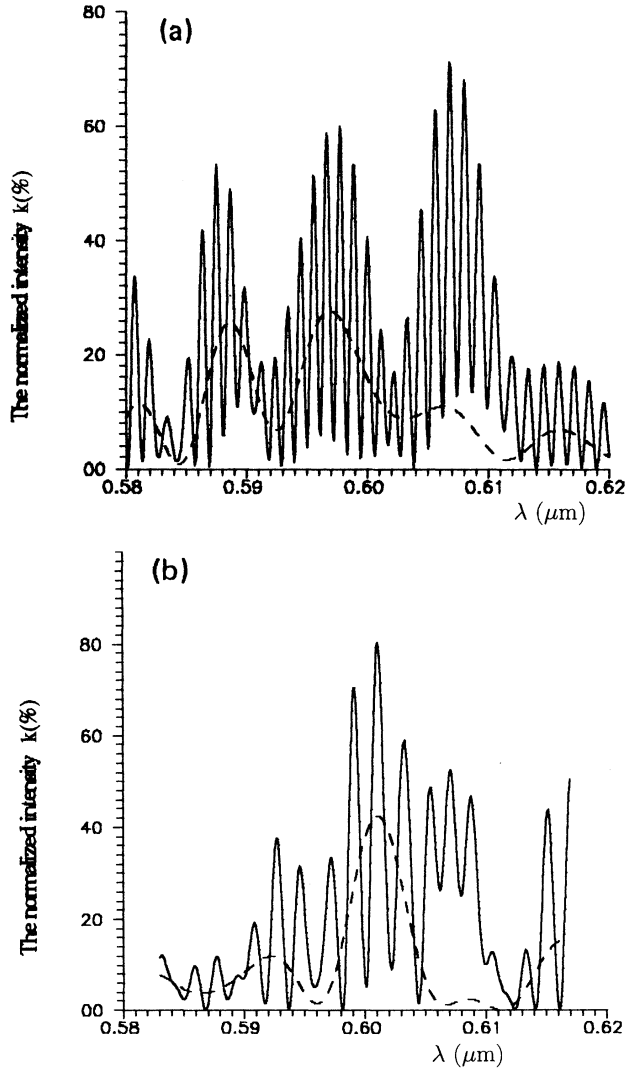

FIG. 13. Calculated spectral distribution of the e-wave intensity after the first block of 200 transverse domains (dashed curves) and the third, 200-domain block (solid curves) for $\theta=6°$. (a) $\bar{d}_1=7.44$ μm, $d_2=6$ mm, $\bar{d}_3=7.49$ μm, $\sigma_1=0.728$ μm, $\sigma_3=0.700$ μm; (b) $\bar{d}_1=7.30$ μm, $d_2=2$ mm, $\bar{d}_3=7.61$ μm, $\sigma_1=0.973$ μm, $\sigma_3=1.042$ μm. All the symbols are the same as in Fig. 12.

caused by the second block of longitudinal domains ($\cong 3$ nm).

But since the block of transverse domains is an active converter and a phase plate simultaneously, then at certain deviations of phase ($\cong \pm\pi$) or wavelength from their central (peak) value, there must be cancellation of the active conversion. That is why the resonant curve $|E_{200}(\lambda)|^2$ passes through zero in the intervals $\lambda \cong 0.594-0.595$ and $0.605-0.606$ μm. At these points the e-wave phase is not determined, and phase jumps are possible (analogous jumps occur in the case of dislocations and branching of the interference fringes observed in interferometry). It follows from Fig. 12(b) that such a situation exits in the range $\lambda \cong 0.605-0.606$ μm. This phase jump, together with the phase modulation caused by the second block of longitudinal domains, breaks the periodicity of the spectral maxima [see Fig. 12(a)]. Effects of this kind are the most probable reason for the observed deviations of the interline distances from their mean values (see Figs. 3 and 4).

The proposed model enables us to develop an approach to the ill-defined inverse problem of determining structure and statistics of domains from the spectra. Indeed, comparing the experimental spectra shown in Figs. 3 and 4 with the results of numerical calculations (Fig. 12) we can make the following conclusions.

First, the existence of equidistant maxima in a wide spectra range indicates that the distribution of transverse-domain thicknesses is wider in the experimental spectra. Second, the interline distance is shorter in experimental spectra, presented in Fig. 3(b), than in the calculated spectra in Fig. 12. So the thickness of the longitudinal block must be increased. Figure 13 shows examples of spectra calculated for different mean values and larger mean square dispersions of domain thicknesses in two transverse blocks. The total number of lines in the computer spectra grows as the structure is considered to be more disordered. The thickness of the longitudinal block in Fig. 13(a) was taken equal to 6 mm instead of 3 mm as for the spectrum in Fig. 12. As a result, the calculated spectrum becomes more similar to the experimental spectrum in Fig. 3(b). On the other hand, the spectrum in Fig. 13(b) was calculated for 2 mm longitudinal-block thickness, and it is similar to the experimental spectrum in Fig. 3(c).

VII. COMPARISON WITH THE EXPERIMENTAL RESULTS

Actually, all parameters, such as domain numbers, mean thicknesses, mean square deviations, and types of domain-thickness statistical distribution, may differ in different blocks. Moreover, the scattering spectra can be formed not only by three domain blocks (triples as in Fig. 10) but by a much larger number of them. We have considered the sequence of only three domain blocks—transverse, longitudinal, and again transverse—because this number of blocks seems to be the minimal block construction that can provide the main observed spectral features. The first transverse block is necessary to create light of orthogonal polarization, since there is only linearly polarized light at the input of the crystal. The second, longitudinal block is to make a phase delay between orthogonally polarized light waves, the delay rapidly varying with the wavelength. The last transverse block is to make interference between two orthogonally polarized beams.

The phase delay is also caused by unresonant domains from transverse blocks. In fact, this delay may be responsible for the fast periodic spectral variations as well. Hence the existence of the longitudinal block is not necessary in the strict sense. But we do not discuss this situation here because actually there is a certain number of longitudinal blocks in each multiply domained sample of KH_2PO_4.

So let us analyze the results of calculations based on the triples model. The examples of calculated spectra are presented in Figs. 12 and 13. Their high sensitivity to slight variations of the domain structure is a point of peculiar interest. Even for the same statistical parameters of the transverse blocks (mean thicknesses and dispersions), there are significant differences in calculated spectra for different realizations. So we could not fit all numerical parameters of the calculated spectrum to achieve an exact agreement with the experimental spectra. At the same time, the main characteristic features of the experimental spectra are also observed in the calculated spectra. Comparing the features of the experimental spectra listed in Sec. III with the results of numerical computation we can make the following conclusions.

(1) A high-contrast dependence on the wavelength and on the deflection angle is observed in the model calculations, the same ways as in the experiment. Interchange of the intensity maxima and minima takes place in the experimental spectra when the crossed polarizer and analyzer become parallel. It follows automatically from the unitarity condition for conversion (4), which is confirmed by relation (5).

(2) In the computer calculations the high sensitivity of the spectra to the domain structure variation has also been observed. Even the interchange of two neighboring transverse layers, for example, of the 180th and 181st, becomes noticeable.

(3) The theory predicts the same order and spectral behavior of line curvatures $\rho(\omega)=d\theta/d\omega$. It seems that subsystems of lines with the same curvature result from light propagation through triples of domains (transverse-longitudinal-transverse) or other, more complicated structures, which also give an almost equidistant system of lines. The overlapping of lines with different curvature is connected with the overlapping of spectra formed by different combinations of such triples. According to model calculations, there must be no energy transfer from one polarization to another at zero angle θ, when light waves are propagating in the XY plane. The question how the set of displaced lines was observed at small angles [see Fig. 4(a)] in some spectra still remains. The reason may be connected with the local disturbance of domain structure in some samples.

(4) The regularity and equidistant character of spectral maxima is quite observable in the calculated spectra. The spectra calculated according to a model of one triple are

not so rich as experimental ones; they do not occupy the whole visible range. But the periodicity of the line position is not ideal also. For example, see the distortions of equidistant character in Fig. 12(a) caused by additional phase modulation in the transverse block.

(5) The increase of the distance between spectral maxima with the wavelength according to Fig. 7(a) follows from the results of numerical calculations too. Increase of the longitudinal block thickness decreases this distance [compare Figs. 13(a) and 13(b)]. Probably this is the reason of the shorter average intermode distances observed in experimental spectra of longer crystals [see Fig. 7(a)].

(6) The high efficiency of energy transfer from waves of one polarization type (*o*) to waves of orthogonal polarization type (*e*) takes place also in the calculated data presented in Figs. 12(a) and 13. The groups of lines obtained in calculations occupy the spectral ranges of the widths appropriate to describe quasiperiodic slow modulation of the average line intensity. The average line intensity is not a constant in the calculated spectra and slightly depends on the wavelength too. The different wide maxima in $\bar{k}$ spectra can be associated with anisotropic diffraction of light on transverse blocks.

So to understand the experimental results it is enough to consider only three domain blocks, a triple. But actually light passes through many different blocks when propagating through the crystal. How does the existence of other domain blocks influence the observable spectra? The key to the answer to this question is the resonant character of the interaction of the different domain systems with light. Different triples of domain blocks work in different spectral ranges, and the resulting spectrum is a superposition of separate spectra formed by such triples.

It is clear from the presented results that the mean domain thicknesses and the statistical characteristics of the first and third transverse blocks need not coincide. It is only necessary that their resonance curves overlap. All domains with unresonant thicknesses, longitudinal blocks being located between these two transverse blocks, play the role of effective phase plates, causing a fast periodic spectral modulation. The spectral dependence of the mean $\bar{k}$ is the result of the superposition of resonant curves of transverse blocks.

The existence of equidistant lines in the spectra follows also from other simple considerations. Let the final block of transverse domains be described by matrix D of dimension 2×2. Then the input and the output fields of this block will be connected by the relationship

$$\begin{bmatrix} O_{\text{out}} \\ E_{\text{out}} \end{bmatrix} = D \begin{bmatrix} O_{\text{in}} \\ E_{\text{in}} \end{bmatrix} . \tag{15}$$

Therefore the output intensity in one of the polarizations (say, *e*) is

$$|E_{\text{out}}|^2 = |D_{21} O_{\text{in}}|^2 + |D_{22} E_{\text{in}}|^2 + 2\,\text{Re}(D_{21} D_{22}^* O_{\text{in}} E_{\text{in}}^*) , \tag{16}$$

where D_{ij} are the matrix elements of D.

Let the variation of wavelength λ lead to the linear growth of phase $\varphi_{\text{in}} = \arg(E_{\text{in}})$, and the rate of this growth be essentially larger than the variation rates of other parameters in Eq. (16) (such a fast phase modulation occurs mainly in the block of longitudinal domains). In this case, according to (16), a spectrum of equidistant lines with harmonic modulation is formed in the wavelength range where only variations of phase φ_{in} can be noticed.

VIII. CONCLUSIONS

The proposed model is able to explain the basic characteristic features of the spectra observed in experiment. High-contrast and nearly equidistant lines, a quasiperiodic envelope of the spectrum, interfering systems of lines—this complicated and emphatic picture of scattering is explained in the framework of a rather simple model. This model is based on the anisotropic and multiply domained nature of the medium. It accounts for the polarization rotation at the borders of transverse domains and for the variation of the phase difference between the orthogonally polarized waves on their way through both types of domains, transverse and longitudinal. A few specific effects require additional consideration, which will be done in further papers.

Having achieved some clarity in the origin of the elastic-scattering spectra, we can try to solve the inverse problem—to determine the domain structure parameters of a multiply domained scattering sample. We also can calculate the dispersion of the principal values of the optical parameters at low temperatures and analyze how the domain structure and the local field affect the crystal parameters. From the viewpoint of applications, we would like to mention that multidomained crystals can be used as controlled high-efficiency polarization filters.[23] Such filters do not need fine optical surface treatment: domain walls are natural high-quality optical devices.

The effects considered in this work are also to be taken into account while studying the inelastic-scattering spectra. For instance, one should consider the influence of the change of selection rules caused by the multiply domained superstructure.[5] The question of quantization of the elementary excitations in media with layer-type multiply domained superstructures of this type is also extremely interesting. We have to mention here the attractive idea of optical-field quantization in multiply domained structures.[24,25]

This consideration of optical effects is useful not only for crystals belonging to the KH_2PO_4 group; the same domain configuration is typical for almost all ferroelectrics of symmetry $mm2$. Some of them have the considered superstructure at room temperatures as well [for instance, $Gd_2(MoO_4)_3$ (Refs. 26,27)]. We hope that the present paper will be a good introduction to the solution of problems connected with the spatial inhomogeneities of multiply domained media.

ACKNOWLEDGMENTS

We are grateful to Professor P. V. Elyutin and Professor D. N. Klyshko for stimulating discussions, and also

to M. V. Chekhova. E. P. Kondratenko, and P. A. Prudkovskii for technical assistance in research. This work is supported in part by grants from the International Laser Center of Moscow State University, and by Grant No. MBQ000 from the International Science Foundation.

APPENDIX

A number of theoretical problems require calculation of integrals of the form

$$I_n=\int_{-\infty}^{\infty}\{e^{-\alpha x^2}/[\beta^2+(x+\gamma)^2]^n\}dx\ , \tag{A1}$$

where α,β,γ are real, $\alpha>0$, and n is an integer. These, for example, are problems relating to spectral analysis. However, as far as we know, this integral is absent in reference literature. Here we present the results of its analytical calculation.

Let us first determine the value of this integral at $n=1$. To do this, we represent the integral in the form

$$I_1=(2\beta)^{-1}\int_{-\infty}^{\infty}\{e^{-\alpha x^2}/[\beta+i(x+\gamma)]\}dx+\text{c.c.}$$

$$=-\beta^{-1}\mathrm{Re}\left\{i\int_{-\infty}^{\infty}[e^{-\alpha x^2}/(x+\gamma-i\beta)]dx\right\}\ , \tag{A2}$$

where c.c. means complex conjugation, i is the imaginary unit, and Re the real part.

Furthermore, we represent (A2) as the sum of two equal terms:

$$I_1=-(2\beta)^{-1}\mathrm{Re}\left\{i\int_{-\infty}^{\infty}[e^{-\alpha x^2}/(x+\gamma-i\beta)]dx\right.$$

$$\left.+i\int_{-\infty}^{\infty}[e^{-\alpha x^2}/(-x+\gamma-i\beta)]\right\}dx\ , \tag{A3}$$

which, in its turn, can be written in the form

$$I_1=\beta^{-1}\mathrm{Re}\left\{(\beta+i\gamma)\int_{-\infty}^{\infty}e^{-\alpha x^2}/[x^2+(\beta+i\gamma)^2]dx\right\}\ , \tag{A4}$$

and this is the already known integral

$$\int_0^{\infty}\{e^{-\alpha x^2}/[x^2+(\beta+i\gamma)^2]\}dx$$

$$=\frac{\pi e^{\alpha(\beta+i\gamma)^2}}{2(\beta+i\gamma)}\{1-\mathrm{erf}[(\beta+i\gamma)\sqrt{\alpha}]\}\ , \tag{A5}$$

where $\mathrm{erf}(u)=2\pi^{-1/2}\int_0^u e^{-t^2}dt$ is the probability integral.

Thus we finally obtain

$$I_1=(\pi/\beta)\mathrm{Re}(\{1-\mathrm{erf}[(\beta+i\gamma)\sqrt{\alpha}]\}e^{\alpha(\beta+i\gamma)^2})\ . \tag{A6}$$

The integral I_n for arbitrary n can be calculated by means of a recurrent relation

$$I_n=-n^{-1}dI_{n-1}/dp\ , \tag{A7}$$

where $p=\beta^2$. For instance, for calculating I_2, one should differentiate Eq. (A6) with respect to β^2, and change the sign.

[1]R. M. Hill and S. K. Ichiki, Phys. Rev. **135**, 1630 (1964).
[2]R. M. Hill, G. F. Hermann, and S. K. Ichiki, J. Appl. Phys. **36**, 3672 (1965).
[3]Y. Takagi and T. Shigenari, Solid State Commun. **11**, 481 (1972).
[4]Y. Takagi and T. Shigenari, J. Opt. Soc. Am. **63**, 995 (1973).
[5]G. Kh. Kitaeva, S. P. Kulik, and A. N. Penin, Sov. Solid State Physics **29**, 2002 (1987).
[6]G. Kh. Kitaeva, S. P. Kulik, and A. N. Penin, Sov. Phys. Solid State **34**, 1841 (1992).
[7]I. P. van der Ziel and N. Blombergen, Phys. Rev. **135**, 1662 (1964).
[8]J. Burfoot and G. Taylor, *Polar Dielectrics and Their Applications* (Macmillan, London, 1979).
[9]F. Iona and G. Shirane, *Ferroelectric Crystals* (Maxilla, New York, 1962).
[10]T. Mitsui and J. Furuichi, Phys. Rev. **90**, 193 (1953).
[11]K. Abbe, J. Phys. Soc. Jpn. **56**, 757 (1987).
[12]J. Bornarel, Ferroelectrics **71**, 255 (1987).
[13]M. V. Chekhova and A. N. Penin, J. Raman Spectrosc. **24**, 581 (1993).
[14]P. V. Elyutin, Usp. Fiz. Nauk (Moscow) **155**, 397 (1988) [Sov. Phys. Usp. **31**, 597 (1988)].
[15]A. Peres, Am. J. Phys. **48**, 931 (1980).
[16]A. Yariv and P. Yeh, *Optical Waves in Crystals* (Wiley-Interscience, New York, 1984).
[17]M. Yamazaki and T. Ogawa, J. Opt. Soc. Am. **56**, 1407 (1966).
[18]R. A. Phillips, J. Opt. Soc. Am. **58**, 629 (1966).
[19]M. Born and E. Wolf, *Principles of Optics* (Pergamon, Oxford, 1964).
[20]A. V. Belinsky and A. S. Chirkin, Sov. J. Quantum Electron. **16**, 593 (1986).
[21]A. V. Belinsky and A. S. Chirkin, Sov. J. Quantum Electron. **16**, 685 (1986).
[22]A. V. Belinsky, Z. A. Tagiev, and A. S. Chirkin, Sov. J. Quantum Electron. **16**, 689 (1986).
[23]J. W. Evans, J. Opt. Soc. Am. **48**, 142 (1958).
[24]D. N. Kylshko, JETP **77**, 222 (1993).
[25]D. N. Klyshko, JETP **78**, 848 (1994).
[26]A. W. Smith and G. Burns, Phys. Rev. **28**, A501 (1969).
[27]A. Kumada, Ferroelectrics **3**, 115 (1972).

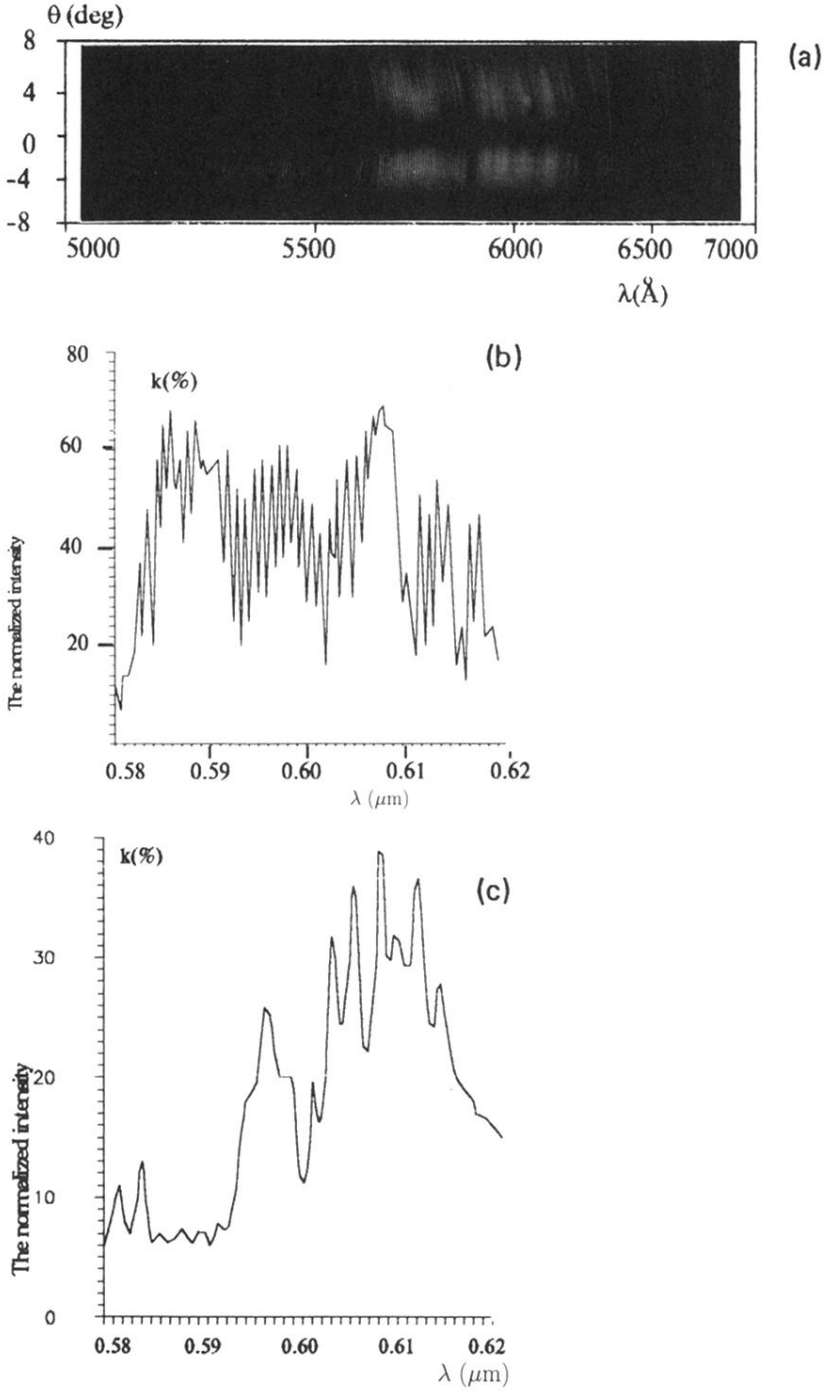

FIG. 3. (a) Photograph of light elastic-scattering spectra in a multiply domained sample (the length $l = 30$ mm). (b), (c) Wavelength dependences of the scattering intensity normalized by the input intensity for spectral range 0.58–0.62 μm: $\theta = 6°$, $l = 30$ mm (b), $\theta = 3°$, $l = 5$ mm (c).

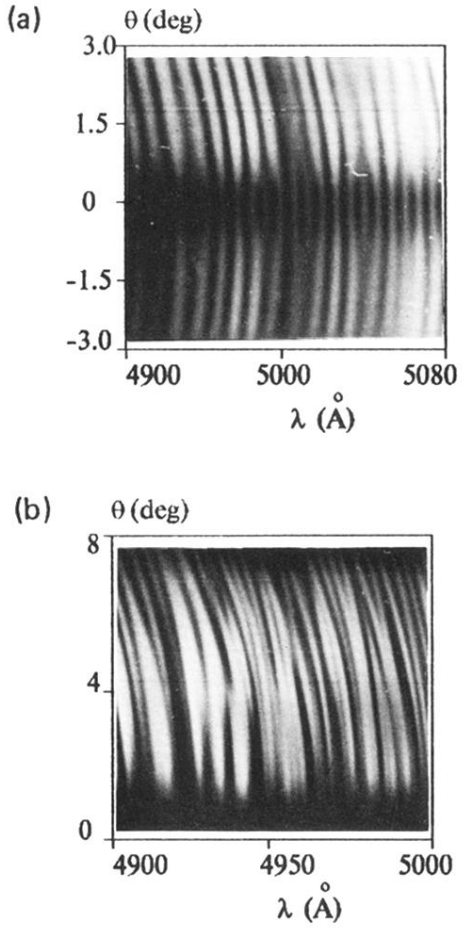

FIG. 4. Fragments of frequency-angular spectra (a) at small angles ($l = 5$ mm) and (b) in the case of mutually repulsive lines ($l = 30$ mm).